

## Article

# Assessing the Effect of Interimplant Distance and Angle on Different Impression Techniques

Berkman Albayrak <sup>1,\*</sup>, İsmail Hakkı Korkmaz <sup>2</sup>, Alvin G. Wee <sup>3</sup>, Cortino Sukotjo <sup>4,\*</sup> and Funda Bayındır <sup>5</sup><sup>1</sup> Department of Prosthodontics, Bahçeşehir University School of Dental Medicine, Istanbul 34349, Turkey<sup>2</sup> Department of Mechanical Engineering, Erzurum Technical University Faculty of Engineering and Architecture, Erzurum 25050, Turkey; ismail.korkmaz@erzurum.edu.tr<sup>3</sup> Division of Prosthodontics—Department of Restorative Sciences, University of Minnesota School of Dentistry, Minneapolis, MN 55455, USA; wee00008@umn.edu<sup>4</sup> Department of Restorative Dentistry, University of Illinois at Chicago College of Dentistry, Chicago, IL 60612, USA<sup>5</sup> Department of Prosthodontics, Atatürk University Faculty of Dentistry, Erzurum 25240, Turkey; bayindirf@atauni.edu.tr

\* Correspondence: berkman.albayrak@dent.bau.edu.tr (B.A.); csukotjo@uic.edu (C.S.); Tel.: +90-537-714-82-93 (B.A.); +1-(617)-272-55-12 (C.S.)

**Abstract:** We aimed to evaluate the trueness of digital and conventional impression techniques based on different angles and distances between implants and the deviation caused by the angle and distance parameters varying between implants. Eight implants were placed in a polyurethane edentulous mandibular model at different angles and distances. After obtaining a 3-dimensional (3D) reference model by using an optical scanner, the model was scanned with three intraoral scanners: Cerec Omnicam (DO), Trios 3 (DT), and Carestream 3500 (DC). Then, the master casts obtained from the conventional impressions (C) were also digitized, and all impression data were imported into reverse engineering software to be compared with the 3D reference model. Distance and angle measurements between adjacent implants were performed, and the data were analyzed with ANOVA–Tukey and Kruskal Wallis tests. The significance level was accepted as  $p < 0.05$ . While DT and C groups gave the best results for high interimplant distances, the trueness of intraoral scanners was found to be superior to the conventional method between closer implants. At higher angulations, the angular trueness of C group was found to be significantly lower. At short distances, digital groups showed superiority, and the trueness of conventional impression decreased with higher angulations.

**Keywords:** angle; digital implant impression; interimplant distance; intraoral scanner; trueness

**Citation:** Albayrak, B.; Korkmaz, İ.H.; Wee, A.G.; Sukotjo, C.; Bayındır, F. Assessing the Effect of Interimplant Distance and Angle on Different Impression Techniques. *Machines* **2022**, *10*, 293. <https://doi.org/10.3390/machines10050293>

Academic Editors: Marek Kočiško and Martin Pollák

Received: 30 March 2022

Accepted: 18 April 2022

Published: 21 April 2022

**Publisher's Note:** MDPI stays neutral with regard to jurisdictional claims in published maps and institutional affiliations.



**Copyright:** © 2022 by the authors. Licensee MDPI, Basel, Switzerland. This article is an open access article distributed under the terms and conditions of the Creative Commons Attribution (CC BY) license (<https://creativecommons.org/licenses/by/4.0/>).

## 1. Introduction

One of the most important criteria for achieving long-term success in implant-supported restorations is to provide a passive fit [1–5]. However, it is not possible to obtain a perfect passive fit due to the dimensional changes that may occur during the impression and subsequent prosthetic production stages [6]. Hence, the initial step in order to obtain the optimum passive fit is to make an accurate conventional or digital impression [7] and transfer the spatial positions of the implants in the bone to the working models where the prosthetic design will be carried out.

Implant impressions use various components. Therefore, the inconsistencies in the junction between the impression copings, the implant, and the analogue can significantly affect the accuracy [8,9]. The amount of these deviations also increases exponentially in cases of multiple implants rather than single implants [10].

In cases with severe alveolar ridge resorption, considering some reasons such as time, cost, patient's age, health condition, and desire, tilted implant placement in non-ideal distances instead of combined treatments such as bone augmentation and sinus

lift operation constitute a serious treatment alternative [11–13]. However, in such cases, implant impression may become complicated, and the trueness of the impression might be compromised [14]. Although splinting of impression copings increases the accuracy, in full arch cases when the angulations exceed  $20^\circ$ , it has been shown that the non-splinted open tray impression is better than the splinted technique [15,16].

The effect of the angulation on the implant impressions was mostly investigated in two implants [17], and the effect of the angulation between each implant was not evaluated by examining the general deviation according to the knowledge of the authors in the complete arch studies performed [2,18–23]. In conventional impressions, deformation can occur even when using polyvinyl siloxane (PVS), an impression material with a high elastic memory, during the removal of the tray from the tilted implants [24,25]. Theoretically, digital implant impressions should not be affected from the angulations, as there is no material deformation or the movement of the impression coping within the impression. However, there are also some studies in the literature that show that digital impression accuracy decreases at angles above 15 to 30 degrees [21,26].

It has been shown that in cases of total and partial edentulism, the accuracy of the impression can vary, taking into account the increased number of implants and the increased distances between the implants [27]. In partial edentulism cases, linear and angular dimensional changes are lower compared to total edentulism, when conventional impression techniques are used [28]. With the increase in the scanned arch distance in the digital impression technique, it becomes difficult to obtain sufficient reference points between the point clouds. As it is not possible to combine the images obtained separately, optical noise and distortions occur in the 3-dimensional (3D) image, or because the software cannot use the surface matching algorithm, it cuts out some of the scanned areas [29]. Therefore, in theory, digital implant impressions are negatively affected by the increase in distance between the scan bodies. In particular, intraoral scanners that work on the principle of combining photos can stick different scan bodies on top of each other if they lose reference points that will continue scanning [30].

The aims of this study are to evaluate the trueness of digital and conventional impression techniques at different angles and distances between implants and the deviation caused by the angle and distance parameters varying between implants. The first hypothesis of this study is as follows: while the conventional method gives better results in areas where the distance between implants is large, the digital method is superior for areas with angulation. The second hypothesis is that the deviation will be higher in the regions where the distance and angulation between the adjacent implants are also high.

## 2. Materials and Methods

Eight implants (Dyna Dental Engineering BV, the Netherlands) (4.2 mm diameter and 11.5 mm length) were placed in a polyurethane edentulous mandible model (Promedius, Poland) at different distances and angles. Implants were inserted to the sites of #47, #44, #43, #41, #33, #34, #35, and #37. The implants were placed at  $40^\circ$ ,  $0^\circ$ ,  $20^\circ$ ,  $0^\circ$ ,  $15^\circ$ ,  $0^\circ$ ,  $0^\circ$ , and  $25^\circ$  angles distally, respectively. All angles were arranged in the distal direction to mimic the distal angulation used in the production of cantilever segmented prosthesis [31].

First, in order to obtain a 3D reference model in which measurements will be made, Ti-base abutments (Dyna Dental Engineering BV, the Netherlands) were first placed on each of the implants. Eight abutment-level scan bodies (Dyna Dental Engineering BV, the Netherlands) were then seated on Ti-base abutments (Figure 1).

Afterwards, the model with the scan bodies was scanned using the Activity 885 Mark 2 Scanner (Smart Optics, Bochum, Germany) with an accuracy of  $6\ \mu\text{m}$  as in previous studies [20,32,33], and the 3D reference model was obtained by exporting the data in standard tessellation language (STL) format to be used in comparisons (Figure 2).

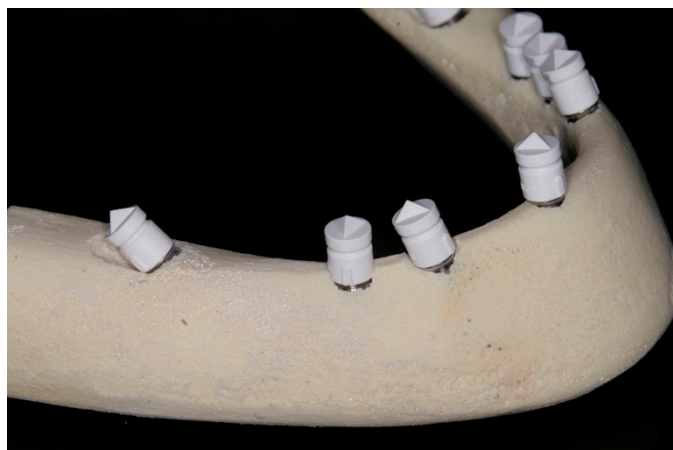


**Figure 1.** Working model with scan bodies attached to implants.

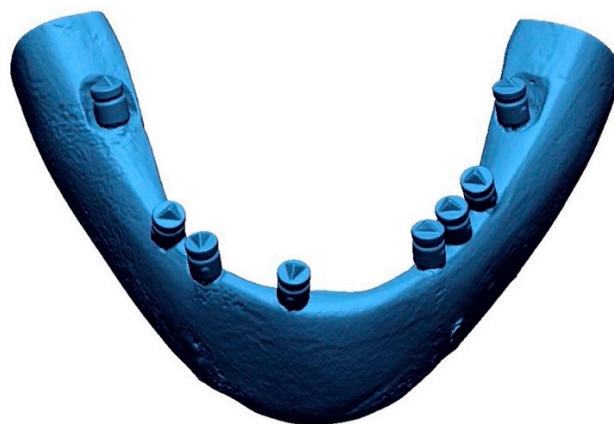


**Figure 2.** Reference 3D model obtained with optical scanner.

The study model was scanned 10 times with each scanner by a single operator before the final scans so that the user could adapt to each of the intraoral scanning systems. Then, starting from area #47 on the right posterior and continuing to the left posterior, scans were performed by following the scanning strategy recommended by the manufacturer of each scanner [34–36].

In the scans performed with the Cerec Omnicam (Dentsply Sirona, Bensheim, Germany), starting from the right posterior region (#47); occlusal, buccal, and lingual surfaces of each scan body were scanned, and the same procedure was continued until the left posterior region (#37). In Trios 3 (3-Shape, Copenhagen, Denmark) scans, scanning that started from the right posterior region occlusally was continued to the left posterior region, followed by scanning of the lingual and buccal surfaces. Unlike these, in Carestream 3500 scans, occlusal imaging of the scan bodies was completed, and then buccal and lingual surfaces were scanned. After each scan, the images were examined and the missing areas were scanned again; the digital impression phase was completed after the meshing procedure. Thus, a total of 30 STL files were obtained, including 10 from three different intraoral scanners.

For the conventional impression phase, eight open tray impression copings were attached to the implants after the removal of the scan bodies and Ti-base abutments. Before each impression, Kerr polyvinyl siloxane (PVS) tray adhesive (KaVo Dental GmbH, Bismarckring, Germany) was applied to the customized impression trays produced according to the model with 3-mm-space thickness. Then, the normal set Elite HD + putty soft and Elite HD + light body (Zhermack SpA, Rovigo, Italy) PVS were placed on the study model with the help of the tray to make single-step impression. After 10 min of setting time of the PVS,

the trays were separated from the model and the analogs were attached to the impression copings. Soft tissue silicone (Zhermack Gingifast Elastic, Zhermack SpA, Rovigo, Italy) was applied to the areas where impression copings were located, and this silicone was allowed set. Afterwards, casting was performed using 150 g GC Fujirock type IV dental stone (GC Corporation, Tokyo, Japan) at a 1:5 powder–liquid ratio using a vacuum mixer. The gypsum was set (2 h) in accordance with the manufacturer’s instructions, and in this phase, all models were kept at room temperature.

Ti-base abutments and scan bodies were placed on the cast models before the measurements were made. All cast models were digitized, and 3D models were obtained using a Straumann 7 Series laboratory scanner (Straumann Group, Basel, Switzerland). In total, 40 STL files were obtained, including 30 from the digital impression group and 10 from the conventional impression group (Figure 3).

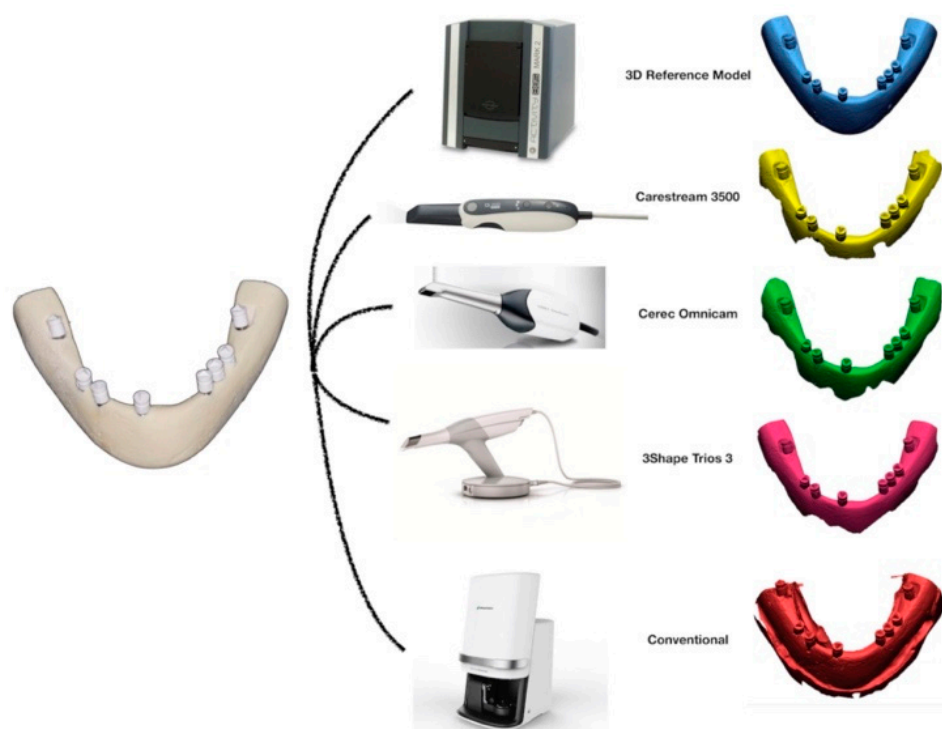
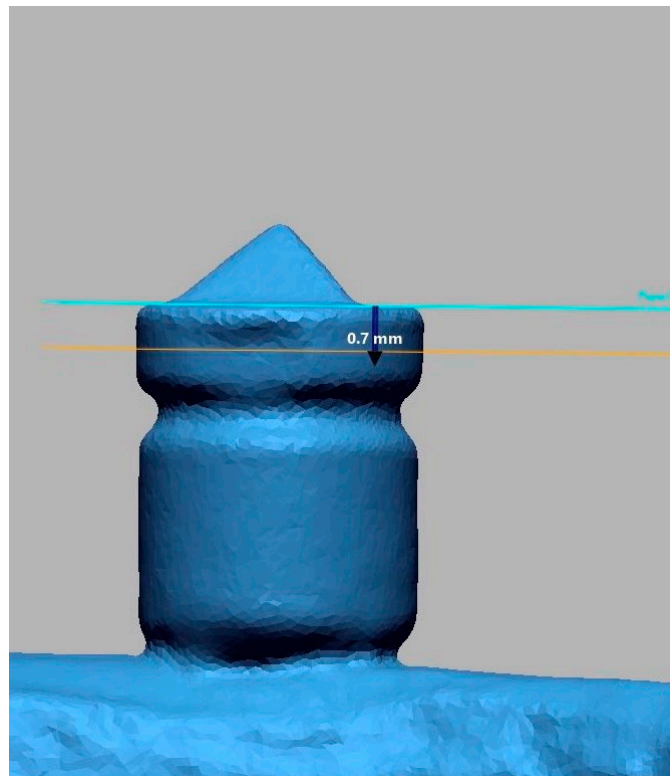


**Figure 3.** Entire impression groups.

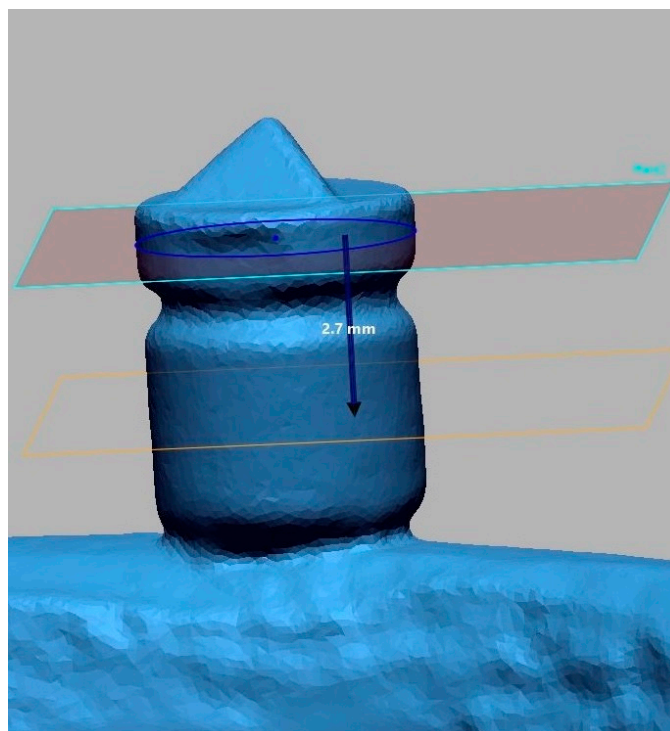
During distance and angle measurements, first, all STL data obtained with the impressions were transferred to Rapidform (INUS Technology Inc., Seoul, South Korea) reverse engineering software. Reference points were determined on the scan bodies in the 3D images where measurements would be made. Two circles (Figure 4c) were formed in the upper and lower cylinders on the scan body, and their centers were determined to be 0.7 and 3.4 mm away from the base of the triangular pyramid with the “point” command (Figure 4a,b).

For all scan bodies in each scan, cartesian  $(x, y, z)$  coordinates of these points were exported from Rapidform in “.txt” format. The coordinates of the reference points of each scan body were determined by using midpoint of the centers of upper and lower circles. The distance between two reference points of  $P_1(x_1, y_1, z_1)$  and  $P_2(x_2, y_2, z_2)$  was calculated by using the following formula:

$$|P_1P_2| = \sqrt{(x_1 - x_2)^2 + (y_1 - y_2)^2 + (z_1 - z_2)^2}$$



(a)



(b)

Figure 4. Cont.



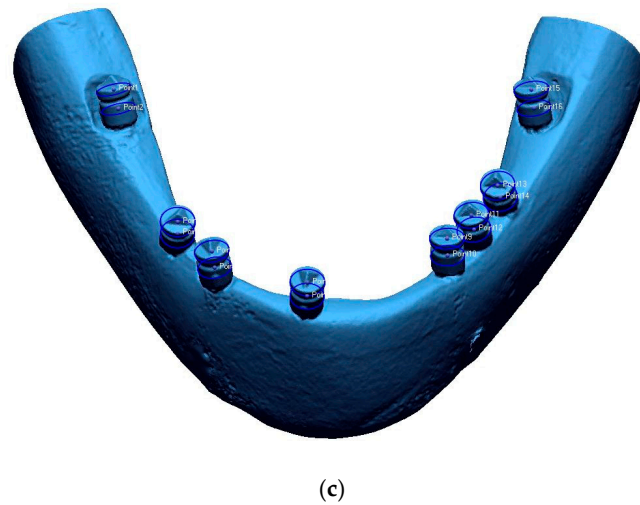


Figure 4. (a) First circle on the scan body, (b) Second circle on the scan body, (c) The centers of the two cross-section circles of all scan bodies.

Distance measurements were made by reference points (P) on scan bodies attached to implants, each located at a different distance. Accordingly, the distances between adjacent scan bodies were determined in both the reference model and the impression groups. (P<sub>1</sub>-P<sub>2</sub>, P<sub>2</sub>-P<sub>3</sub>, P<sub>3</sub>-P<sub>4</sub>, P<sub>4</sub>-P<sub>5</sub>, P<sub>5</sub>-P<sub>6</sub>, P<sub>6</sub>-P<sub>7</sub>, P<sub>7</sub>-P<sub>8</sub>).

Angle measurements were made with the following formula:

$$l_1 = \frac{x - x_1}{a_1} = \frac{y - y_1}{b_1} = \frac{z - z_1}{c_1}; l_2 = \frac{x - x_2}{a_2} = \frac{y - y_2}{b_2} = \frac{z - z_2}{c_2}$$

$$\cos \varphi = \frac{\vec{s}_1 \cdot \vec{s}_2}{|\vec{s}_1| \cdot |\vec{s}_2|} = \frac{a_1 \cdot a_2 + b_1 \cdot b_2 + c_1 \cdot c_2}{\sqrt{a_1^2 + b_1^2 + c_1^2} \cdot \sqrt{a_2^2 + b_2^2 + c_2^2}}$$

In the angle measurements, the lines passing through the centers of the circles formed on the scan bodies were used. In the angle measurement formulation, the lines were found according to the points determined (l<sub>1</sub>, l<sub>2</sub>) and their direction vectors ( $\vec{s}_1, \vec{s}_2$ ). A vector ( $\vec{s}_s$ ) was defined for each scan body, taking into account the center points of scan body's drawn circles. In a Cartesian coordinate system, a vector with a component "x, y, z" can be calculated with this formula: ( $\vec{s}_s$ ) = ai + bj + ck. The letters "a,b,c" are the coefficients that express the direction magnitude. Consequently, the angle between the reference scan body ( $\vec{s}_{s_1}$ ) and the other scan body ( $\vec{s}_{s_2}$ ) was defined in this way and it was calculated with the above formulation ( $\vec{s}_{s_1} \vec{s}_{s_2}, \vec{s}_{s_1} \vec{s}_{s_3}, \vec{s}_{s_1} \vec{s}_{s_4}, \vec{s}_{s_1} \vec{s}_{s_5}, \vec{s}_{s_1} \vec{s}_{s_6}, \vec{s}_{s_1} \vec{s}_{s_7}, \vec{s}_{s_1} \vec{s}_{s_8}$ ).

In this study, starting from the right posterior region (#47), all eight scan bodies were numbered from P1 to P8. Distance (D) is expressed by adjacent scan body numbers: D<sub>1-2</sub>, D<sub>2-3</sub>, D<sub>3-4</sub>, D<sub>4-5</sub>, D<sub>5-6</sub>, D<sub>6-7</sub>, D<sub>7-8</sub>. Angle (A) is also expressed by adjacent scan body numbers: A<sub>1-2</sub>, A<sub>2-3</sub>, A<sub>3-4</sub>, A<sub>4-5</sub>, A<sub>5-6</sub>, A<sub>6-7</sub>, A<sub>7-8</sub>. By determining the deviation of the data of a total of four impression groups with respect to the reference model, comparisons were made between both the impression groups and different adjacent implants.

The distance and angle measurement data were analyzed with IBM SPSS Statistics 20.0 Release Notes program. First, the normality of the data was investigated with the Shapiro–Wilk test. The difference between the mean values of the variables with normal distribution was analyzed by one-way ANOVA, and Tukey's multiple comparison test was used to determine the differences between each group. The difference between the median values of the variables with non-normal distribution was analyzed by the Kruskal–Wallis test. First, the distance and angle deviations between the different adjacent implants of

the impression groups were compared, and then the digital and conventional impression performances of the double-adjacent implants were evaluated. All statistical analyses were performed after taking absolute values of the data, and 0.05 was used as the level of significance.

### 3. Results

The first comparison was made between different impression groups: Cerec Omnicam (DO), Trios 3 (DT), Carestream 3500 (DC), and conventional (C).

#### 3.1. Comparison of Distance Trueness

In the distance (D) parameter, there was no significant difference only in D<sub>1-2</sub>, while a significant difference was found in all other distance deviations (Table 1). DT and C groups showed less deviation in the D<sub>4-5</sub> and D<sub>7-8</sub> regions, where the distance between the implants was greater than that in the other groups. In the regions where the distances between the implants were close (D<sub>2-3</sub>, D<sub>3-4</sub>, D<sub>5-6</sub>, D<sub>6-7</sub>) the conventional group showed the highest deviation, while the digital impression groups gave better results.

**Table 1.** Distance deviations of each impression group between adjacent implants.

	DO		DT		DC		C		Test Statistics	p
	Mean ± SD	Median (Min–Max)	Mean ± SD	Median (Min–Max)	Mean ± SD	Median (Min–Max)	Mean ± SD	Median (Min–Max)		
D <sub>1-2</sub> *	0.35 ± 0.21	0.32 (0.06–0.73) <sup>b</sup>	0.5 ± 0.3	0.45 (0.16–1.18) <sup>ab</sup>	0.5 ± 0.43	0.38 (0.15–1.54) <sup>b</sup>	1.48 ± 0.78	1.33 (0.27–3.02) <sup>a</sup>	15,511	0.001
D <sub>2-3</sub> *	0.25 ± 0.16	0.22 (0.01–0.55) <sup>a</sup>	0.44 ± 0.36	0.32 (0.08–1.01) <sup>a</sup>	0.73 ± 0.46	0.73 (0.1–1.45) <sup>a</sup>	1.72 ± 1.41	1.43 (0.47–5.05) <sup>b</sup>	17,118	0.001
D <sub>3-4</sub> *	0.42 ± 0.37 <sup>a</sup>	0.41 (0.03–1.24)	0.37 ± 0.27 <sup>a</sup>	0.28 (0.03–0.74)	0.73 ± 0.43 <sup>ab</sup>	0.63 (0.08–1.41)	1.19 ± 0.83 <sup>b</sup>	1.12 (0.18–2.74)	5197	0.025
D <sub>4-5</sub> *	1.18 ± 1.17	0.6 (0.03–3.03)	0.35 ± 0.28	0.22 (0.12–0.97)	0.51 ± 0.48	0.43 (0.08–1.52)	0.72 ± 0.74	0.57 (–0.19–2.26)	3773	0.287
D <sub>5-6</sub> *	0.44 ± 0.3 <sup>a</sup>	0.41 (0.07–0.99)	0.81 ± 0.26 <sup>ab</sup>	0.82 (0.53–1.27)	0.69 ± 0.37 <sup>ab</sup>	0.84 (0.07–1.11)	1.39 ± 0.86 <sup>b</sup>	1.76 (0.19–2.7)	6255	0.011
D <sub>6-7</sub> *	1.16 ± 0.25	1.25 (0.77–1.49) <sup>b</sup>	0.8 ± 0.25	0.76 (0.44–1.16) <sup>b</sup>	0.18 ± 0.19	0.12 (0.01–0.53) <sup>a</sup>	0.79 ± 0.6	0.79 (0.09–1.62) <sup>b</sup>	20,540	0.000
D <sub>7-8</sub> *	0.68 ± 0.36 <sup>b</sup>	0.7 (0.07–1.25)	0.37 ± 0.3 <sup>ab</sup>	0.29 (0.01–0.89)	0.32 ± 0.2 <sup>a</sup>	0.3 (0.01–0.65)	0.39 ± 0.3 <sup>ab</sup>	0.28 (0.03–0.96)	3149	0.037

\* D refers to distance deviations, and the numbers refer to adjacent implant pairs. The letters “a” and “b” indicate statistically significant difference at  $p < 0.05$  within each row comparison.

#### 3.2. Comparison of Angle Trueness

In the angle (A) parameter, it was determined that there was a significant difference between the groups for all angle deviations, except for A<sub>4-5</sub>, which had an angulation of 15°. In the A<sub>1-2</sub> region, where the angulation of 40° was the highest, C group deviated significantly more than in the DC and DO groups; in the A<sub>2-3</sub> and A<sub>3-4</sub> regions, which also had 20° angulation, the C group had the lowest performance at a significant level. In the parallel placed implant area, A<sub>6-7</sub>, DC had significantly better results compared to other groups, but there was no significant difference between other digital and conventional impression groups (Table 2).

**Table 2.** Angle deviations of each impression group between adjacent implants.

	DO		DT		DC		C		Test Statistics	p
	Mean ± SD	Median (Min–Max)	Mean ± SD	Median (Min–Max)	Mean ± SD	Median (Min–Max)	Mean ± SD	Median (Min–Max)		
A <sub>1-2</sub> *	0.17 ± 0.37	0.05 (0.01–1.23)	0.06 ± 0.02	0.07 (0.01–0.09)	0.05 ± 0.06	0.03 (0–0.19)	0.05 ± 0.03	0.05 (0.02–0.1)	4210	0.240
A <sub>2-3</sub> *	0.01 ± 0	0 (0–0.01) <sup>a</sup>	0.01 ± 0.01	0.01 (0–0.03) <sup>a</sup>	0.01 ± 0.01	0.01 (0–0.03) <sup>a</sup>	0.13 ± 0.06	0.11 (0.06–0.27) <sup>b</sup>	25,948	0.000
A <sub>3-4</sub> *	0.02 ± 0.01 <sup>b</sup>	0.02 (0–0.03)	0.02 ± 0.01 <sup>b</sup>	0.02 (0–0.03)	0.06 ± 0.03 <sup>a</sup>	0.05 (0.02–0.13)	0.08 ± 0.05 <sup>a</sup>	0.06 (0.01–0.16)	9410	0.001
A <sub>4-5</sub> *	0.21 ± 0.4	0.05 (0–1.27) <sup>ab</sup>	0.03 ± 0.01	0.03 (0–0.04) <sup>b</sup>	0.23 ± 0.31	0.16 (0–1.11) <sup>a</sup>	0.06 ± 0.05	0.04 (0.01–0.15) <sup>ab</sup>	12,022	0.007
A <sub>5-6</sub> *	0.03 ± 0.01 <sup>a</sup>	0.03 (0.01–0.04)	0.01 ± 0.01 <sup>b</sup>	0.01 (0–0.02)	0.03 ± 0.01 <sup>a</sup>	0.03 (0.02–0.03)	0.09 ± 0.08 <sup>a</sup>	0.07 (0–0.22)	8803	0.000
A <sub>6-7</sub> *	0.01 ± 0.01 <sup>a</sup>	0.01 (0–0.02)	0.01 ± 0.01 <sup>a</sup>	0.01 (0–0.03)	0.01 ± 0 <sup>a</sup>	0.01 (0–0.02)	0.02 ± 0.01 <sup>b</sup>	0.02 (0–0.05)	7397	0.001
A <sub>7-8</sub> *	0.04 ± 0.01	0.04 (0.01–0.06) <sup>ab</sup>	0.01 ± 0.01	0.01 (0–0.02) <sup>b</sup>	0.09 ± 0.02	0.09 (0.07–0.13) <sup>ab</sup>	0.02 ± 0.02	0.01 (0–0.07) <sup>b</sup>	27,985	0.000

\* A refers to angle deviations, and the numbers refer to adjacent implant pairs. The letters “a” and “b” indicate statistically significant difference at  $p < 0.05$  within each row comparison.

#### 3.3. Effects of Distance and Angle Parameters on Different Impressions

Regardless of the impression groups, when the distance and angle deviations between the adjacent implants were compared, while a significant difference was detected between the groups in the deviation parameter ( $p = 0.00$ ) (Figure 5), no significant difference was found between the groups in the angular deviation ( $p = 0.067$ ) (Figure 6).

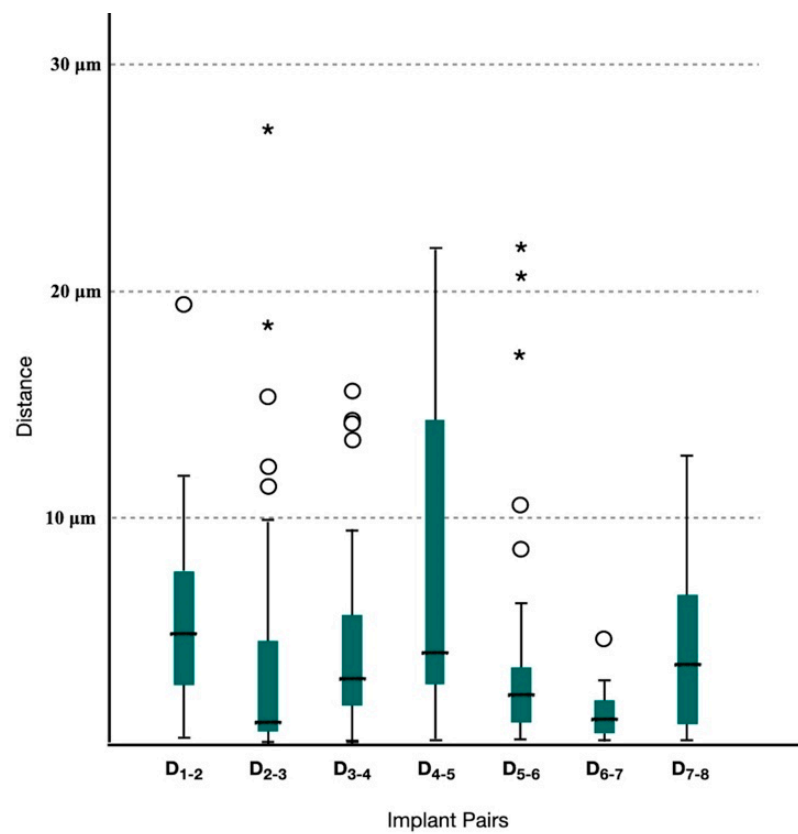


Figure 5. The distance deviations of implant pairs. \* and ○ state outliers.

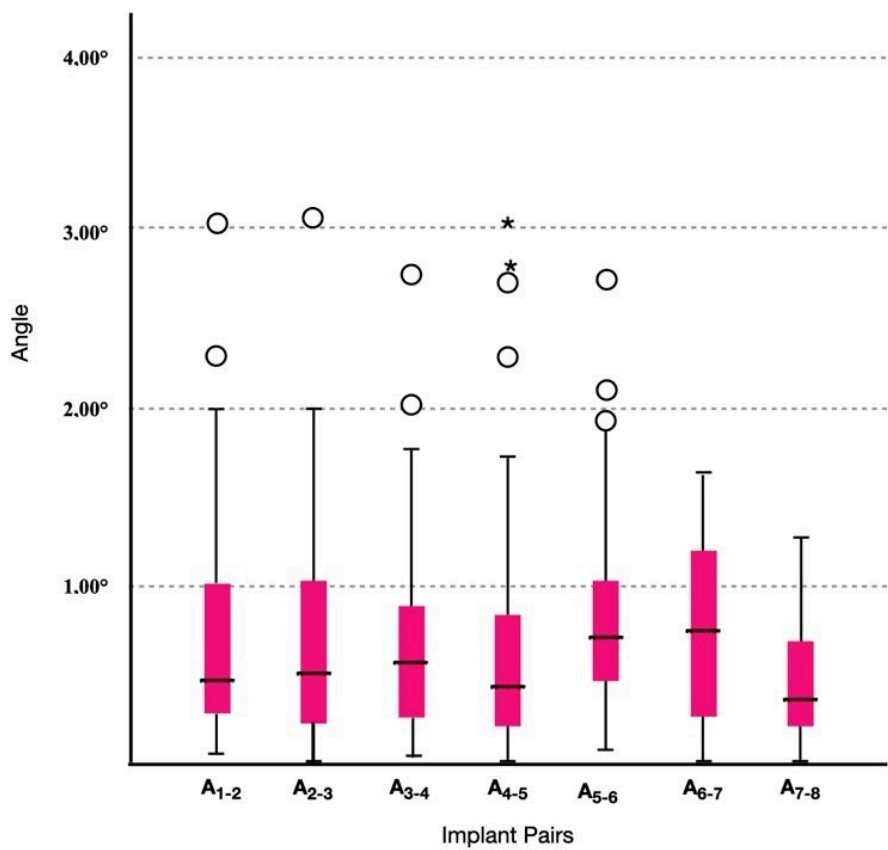


Figure 6. The angular deviations of implant pairs. \* and ○ state outliers.



In D<sub>6-7</sub> and D<sub>2-3</sub>, where the distance between implants was the lowest, the distance deviation was significantly the lowest, followed by D<sub>5-6</sub>, which also did not have any edentulous area. These regions were followed by D<sub>3-4</sub> and D<sub>7-8</sub> with one missing tooth, while the D<sub>4-5</sub> and D<sub>1-2</sub> regions, where the body distance was more than one tooth, were the areas where deviation was detected the most (Table 3).

**Table 3.** Distance deviations between adjacent implants for entire impression groups.

	Mean ± SD	Median (Min–Max)
D <sub>1-2</sub>	0.08 ± 0.19	0.05 (0–1.22) <sup>d</sup>
D <sub>2-3</sub>	0.04 ± 0.06	0.01 (0–0.27) <sup>ab</sup>
D <sub>3-4</sub>	0.04 ± 0.04	0.03 (0–0.16) <sup>c</sup>
D <sub>4-5</sub>	0.13 ± 0.26	0.04 (0–1.27) <sup>cd</sup>
D <sub>5-6</sub>	0.04 ± 0.05	0.02 (0–0.22) <sup>b</sup>
D <sub>6-7</sub>	0.01 ± 0.01	0.01 (0–0.05) <sup>a</sup>
D <sub>7-8</sub>	0.04 ± 0.04	0.04 (0–0.13) <sup>c</sup>
	<b>Test Statistics</b>	<b>p</b>
	52.508	0.000

The letters “a”, “b”, “c” and “d” indicate statistically significant difference at  $p < 0.05$  within each column comparison.

#### 4. Discussion

In the present study, the impressions of the scan bodies at different angles and distances were made with different techniques and different intraoral scanners, and the performances were compared. The deviation amounts of these angle and distance differences on the impressions were evaluated.

According to the results, the first hypothesis of the study that the conventional impression technique would give better results at points where the distance increased and digital impression technique would give better results at points where the angle increased was partially rejected. Intraoral scanners showed superiority over conventional impression in four regions where the distances between scan bodies were short, while Trios 3 was the group that showed the least deviation with the conventional group in two regions with increased distance. In addition, in areas with high angulation such as 40° and 20°, C was the group that showed the most deviation, as expected, while Cerec Omnicam showed the worst performance in a region with 25° angulation.

As with the effect of the edentulous space distance between implants on digital impression trueness [18,37–39], its effects on digital and conventional impressions have been studied in a comparative way in many studies [19,40]. As a result of the study conducted on two different models with six and eight implants, Tan et al. [19] stated that the reduction of the distance between the implants increased the digital impression accuracy, while the conventional impression technique was not affected by this parameter. Schmidt et al. [40] revealed that the deviation that occurs in extent increases with the length of the scanning distance. Likewise, Thanasisuebwong et al. [37] stated that as the edentulous space between the two implants increased, the accuracy of the Trios 3 and Cerec Omnicam scanners decreased. In line with this research, while the largest deviations were observed in the D1-2, D4-5, and D7-8 regions in the digital impression groups, this situation was not observed in the conventional group in the present study.

The accuracy of the impressions made on angled implants has been examined in many studies [2,14,18,22,25,26,41] due to the problems experienced in removing the impression components away from the mouth and transferring them to the master cast. The fact that there is no material deformation and the impression components do not move in digital impressions makes the use of intraoral scanners for angled implants more ideal, theoretically [41]. In this study, digital groups performed better than the conventional in angulations such as 40° and 20°, which support this argument, while DC was the group with the highest deviation in the A<sub>7-8</sub> region with 25°. In a study conducted by Lin et al. [22], while the angulation between implants did not affect the conventional impression accuracy,

it has been reported that it influences the digital impression, but the increase in angulation and deviation did not show a linear ratio. On the other hand, Gimenez et al. [26] stated that angulations had no effect on the digital impression accuracy as a result of the study they carried out on a full arch model including two implants with angulation of 30° and four parallel implants.

In the current study, the deviations between adjacent implants at different distances and angles were evaluated, and impressions with high trueness values were obtained in the D<sub>2-3</sub> and D<sub>6-7</sub> regions where the distance was short. In the D<sub>1-2</sub> and D<sub>4-5</sub> regions with two missing teeth in the pontic region, the highest deviation in the distance parameter was found in the impression groups. While these data support the second hypothesis of the study, no significant difference was detected in the angular deviations between adjacent implants. Therefore, the second hypothesis that the deviation would increase with advancing angulation and distance was also partially rejected.

Intraoral scanners must not lose the reference points they use during imaging so that they can take images of small areas and stitch them together to create all the data correctly [26]. In this study, various pauses were encountered in digital impressions, especially during the scanning of edentulous areas, and the impression was continued by returning and ensuring that the scanner caught the reference point. In these regions, it is predicted that the errors that may occur during the stitching of the newly acquired images with the previous ones by the software increase the deviation. On the contrary, in angled implants, it was observed that the system could easily distinguish the relevant scan body from the others and the scanning could be continued more easily. It is likely that this situation will enable the digital technique to outperform the conventional technique in angled implants.

Some researchers state that one of the factors that negatively affect digital measurement clarity is the positioning of the scanned implants at the chin curvature in the anterior region, rather than being on a straight line [42,43]. However, in the current study, similar deviation values were detected in posterior regions of D<sub>1-2</sub> and D<sub>7-8</sub>, such as the D<sub>4-5</sub> region located at the curvature. The measurement technique can also affect the trueness values. In some studies, the study groups and the reference model were superimposed with the “best-fit alignment” technique [18,37], but some researchers advocate comparing distance and angle measurements between the reference model and other impression groups separately [21,44]. In the present study, the deviation values were obtained by comparing the distance and angle measurements done firstly on the reference model and then on the study groups.

Since this *in vitro* study was carried out on an artificial jaw model, it is not possible to reflect exactly the patient and mucosal movements that can be encountered on a digital impression. Therefore, it is important to evaluate the existing data together with future *in vivo* studies, in terms of clinical success to be achieved in implant impressions. In addition, the negative effects of oral fluids such as saliva and blood on the imaging of intraoral scanners could not be reflected. It will be useful to investigate the accuracy of intraoral scanners in long edentulous spans by adding components that will create a reference for the scanner.

## 5. Conclusions

Within the limitations of this *in vitro* study, it has been determined that digital impression gave better results in areas where the distance between the implants is shorter. With the increase in the distance, the Trios 3 scanner had the highest trueness with the conventional group. The use of Cerec Omnicam and Carestream 3500 scanners was reliable in areas where the distance was shorter between implants. In angular deviation, with the decrease in the performance of the conventional technique compared to the digital impression in the areas where the angle increases, a similar consistency was not found.

**Author Contributions:** Conceptualization, B.A., A.G.W., C.S. and F.B.; methodology, B.A., A.G.W.; İ.H.K., C.S. and F.B.; formal analysis, B.A., İ.H.K., C.S. and F.B.; investigation and data, B.A., İ.H.K., C.S. and F.B.; writing—original draft preparation, B.A. and İ.H.K.; writing—review and editing, B.A.,

A.G.W., C.S. and F.B.; supervision, A.G.W., C.S. and F.B.; project administration: C.S. and F.B. All authors have read and agreed to the published version of the manuscript.

**Funding:** This research received no external funding.

**Data Availability Statement:** Not applicable.

**Acknowledgments:** The authors thank the Dyna Dental Company for supplying all implant components and Zhermack Dental and GC Corporation for their support in terms of impression and cast materials. This study was partially supported by Atatürk University scientific research project. PRJ2015/434.

**Conflicts of Interest:** We wish to confirm that there are no known conflicts of interest associated with this publication and there has been no significant financial support for this work that could have influenced its outcome.

## References

- Moreno, A.; Gimenez, B.; Ozcan, M.; Pradies, G. A clinical protocol for intraoral digital impression of screw-retained CAD/CAM framework on multiple implants based on wavefront sampling technology. *Implant Dent.* **2013**, *22*, 320–325. [[CrossRef](#)] [[PubMed](#)]
- Richi, M.W.; Kurtulmus-Yilmaz, S.; Ozan, O. Comparison of the accuracy of different impression procedures in case of multiple and angulated implants: Accuracy of impressions in multiple and angulated implants. *Head Face Med.* **2020**, *16*, 9. [[CrossRef](#)] [[PubMed](#)]
- Bacchi, A.; Consani, R.L.; Mesquita, M.F.; Dos Santos, M.B. Effect of framework material and vertical misfit on stress distribution in implant-supported partial prosthesis under load application: 3-D finite element analysis. *Acta Odontol. Scand.* **2013**, *71*, 1243–1249. [[CrossRef](#)] [[PubMed](#)]
- Hanif, A.; Qureshi, A. Complications in implant dentistry. *Eur. J. Dent.* **2017**, *11*, 135–140. [[CrossRef](#)]
- Taylor, T.D.; Agar, J.R.; Vogiatzi, T. Implant prosthodontics: Current perspective and future directions. *Int. J. Oral Maxillofac. Implant.* **2000**, *15*, 66–75.
- Abduo, J.; Bennani, V.; Waddell, N.; Lyons, K.; Swain, M. Assessing the fit of implant fixed prostheses: A critical review. *Int. J. Oral Maxillofac. Implant.* **2010**, *25*, 506–515.
- Wee, A.G. Comparison of impression materials for direct multi-implant impressions. *J. Prosthet. Dent.* **2000**, *83*, 323–331. [[CrossRef](#)]
- Kim, S.; Nicholls, J.I.; Han, C.H.; Lee, K.W. Displacement of implant components from impressions to definitive casts. *Int. J. Oral Maxillofac. Implant.* **2006**, *21*, 747–755.
- Kwon, J.H.; Son, Y.H.; Han, C.H.; Kim, S. Accuracy of implant impressions without impression copings: A three-dimensional analysis. *J. Prosthet. Dent.* **2011**, *105*, 367–373. [[CrossRef](#)]
- Kim, K.R.; Seo, K.Y.; Kim, S. Conventional open-tray impression versus intraoral digital scan for implant-level complete-arch impression. *J. Prosthet. Dent.* **2019**, *122*, 543–549. [[CrossRef](#)]
- Asawa, N.; Bulbule, N.; Kakade, D.; Shah, R. Angulated implants: An alternative to bone augmentation and sinus lift procedure: Systemic review. *J. Clinic Diag. Res.* **2015**, *9*, 10–13. [[CrossRef](#)] [[PubMed](#)]
- Patel, M.P.; Anilkumar, S.; Chaukramath, R.; Gopalkrishnan, S. Rehabilitation of edentulous maxillary arch with implant-assisted fixed complete prosthesis using multi-unit straight and angulated abutments. *Eur. J. Prosthodont.* **2016**, *4*, 37–40. [[CrossRef](#)]
- Oltra, D.P.; Marti, E.C.; Ali, J.A.; Diago, M.P. Rehabilitation of the atrophic maxilla with tilted implants: Review of literature. *J. Oral Implantol.* **2013**, *39*, 625–632. [[CrossRef](#)] [[PubMed](#)]
- Gintaute, A.; Papatriantafyllou, N.; Aljehani, M.; Att, W. Accuracy of computerized and conventional impression-making procedures of straight and tilted dental implants. *Int. J. Esthet. Dent.* **2018**, *13*, 550–565.
- Alikhasi, M.; Siadat, H.; Nasirpour, A.; Hasanzade, M. Three-dimensional accuracy of digital impression versus conventional method: Effect of implant angulation and connection type. *Int. J. Dent.* **2018**, *2018*, 3761750. [[CrossRef](#)]
- Ribeiro, P.; Herrero-Climent, M.; Díaz-Castro, C.; Ríos-Santos, J.; Padrós, R.; Mur, J.; Falcão, C. Accuracy of implant casts generated with conventional and digital Impressions—An in vitro study. *Int. J. Environ. Res. Public Health* **2018**, *15*, 1599. [[CrossRef](#)]
- Shim, J.S.; Ryu, J.J.; Shin, S.W.; Lee, J.Y. Effects of implant angulation and impression coping type on the dimensional accuracy of impressions. *Implant Dent.* **2015**, *24*, 726–729. [[CrossRef](#)]
- Pereira, A.L.C.; De Freitas, R.F.C.P.; Campos, M.D.F.T.P.; Tôrres, A.C.S.P.; De Medeiros, A.K.B.; Carreiro, A.D.F.P. Trueness of a device for intraoral scanning to capture the angle and distance between implants in edentulous mandibular arches. *J. Prosthet. Dent.* **2021**, *in press*. [[CrossRef](#)]
- Tan, M.Y.; Hui Xin Yee, S.; Wong, K.M.; Tan, Y.H.; Tan, K.B.C. Comparison of three-dimensional accuracy of digital and conventional implant impressions: Effect of interimplant distance in an edentulous arch. *Int. J. Oral Maxillofac. Implant.* **2019**, *34*, 366–380. [[CrossRef](#)]
- Amin, S.; Weber, H.P.; Finkelman, M.; El Rafie, K.; Kudara, Y.; Papaspyridakos, P. Digital vs. conventional full-arch implant impressions: A comparative study. *Clin. Oral Implant. Res.* **2017**, *28*, 1360–1367. [[CrossRef](#)]

21. Gimenez, B.; Özcan, H.; Martínez-Rus, F.; Pradiés, L. Accuracy of a digital impression system based on active wavefront sampling technology for implants considering operator experience, implant angulation, and depth. *Clin. Implant. Dent. Relat. Res.* **2015**, *17*, e54–e64. [CrossRef] [PubMed]
22. Lin, W.S.; Harris, B.T.; Elathamna, E.N.; Abdel-Azim, T.; Morton, D. Effect of implant divergence on the accuracy of definitive casts created from traditional and digital implant-level impressions: An in vitro comparative study. *Int. J. Oral Maxillofac. Implant.* **2015**, *30*, 102–109. [CrossRef] [PubMed]
23. Gimenez, B.; Özcan, H.; Martínez-Rus, F.; Pradiés, L. Accuracy of a digital impression system based on active triangulation technology with blue light for implants: Effect of clinically relevant parameters. *Implant Dent.* **2015**, *24*, 498–504. [CrossRef] [PubMed]
24. Sorrentino, R.; Gherlone, E.F.; Calesini, G.; Zarone, F. Effect of implant angulation, connection length, and impression material on the dimensional accuracy of implant impressions: An in vitro comparative study. *Clin. Implant. Dent. Relat. Res.* **2010**, *12*, 63–76. [CrossRef]
25. Kurtulmuş-Yılmaz, S.; Ozan, O.; Özçelik, T.B.; Yağız, A. Digital evaluation of the accuracy of impression techniques and materials in angulated implants. *J. Dent.* **2014**, *42*, 1551–1559. [CrossRef]
26. Gimenez, B.; Özcan, M.; Martínez-Rus, F.; Pradies, G. Accuracy of a digital impression system based on parallel confocal laser technology for implants with consideration of operator experience and implant angulation and depth. *Int. J. Oral Maxillofac. Implant.* **2014**, *29*, 853–862. [CrossRef]
27. Ma, J.; Rubenstein, J.E. Complete arch implant impression technique. *J. Prosthet. Dent.* **2012**, *107*, 405–410. [CrossRef]
28. Flügge, T.; Van Der Meer, W.J.; Gonzalez, B.M.; Vach, K.; Wismeijer, D.; Wang, P. The accuracy of different dental impression techniques for implant-supported dental prostheses: A systematic review and meta-analysis. *Clin. Oral Implant. Res.* **2018**, *29*, 374–392. [CrossRef]
29. Gimenez, B.; Pradies, G.; Martínez-Rus, F.; Özcan, M. Accuracy of two digital implant impression systems based on confocal microscopy with variations in customized software and clinical parameters. *Int. J. Oral Maxillofac. Implant.* **2015**, *30*, 56–64. [CrossRef]
30. Flügge, T.; Att, W.; Metzger, M.; Nelson, K. A Novel method to evaluate precision of optical implant impressions with commercial scan bodies—An experimental approach. *J. Prosthodont.* **2017**, *26*, 34–41. [CrossRef]
31. Drago, C. Ratios of cantilever lengths and anterior-posterior spreads of definitive hybrid full-arch, screw-retained prostheses: Results of a clinical study. *J. Prosthodont.* **2018**, *27*, 402–408. [CrossRef] [PubMed]
32. Papaspyridakos, P.; Rajput, N.; Kudara, Y.; Weber, H.P. Digital workflow for fixed implant rehabilitation of an extremely atrophic edentulous mandible in three appointments. *J. Esthet. Restor. Dent.* **2017**, *29*, 178–188. [CrossRef] [PubMed]
33. Marghalani, A.; Weber, H.P.; Finkelman, M.; Kudara, Y.; El Rafie, K.; Papaspyridakos, P. Digital versus conventional implant impressions for partially edentulous arches: An evaluation of accuracy. *J. Prosthet. Dent.* **2018**, *119*, 574–579. [CrossRef] [PubMed]
34. CS 3500 Real-Time Full Arch Scan I Streamhealth Dental. Available online: <https://www.youtube.com/watch?v=sMEykCIRBkI&t=31s> (accessed on 29 November 2021).
35. Tutorial: CEREC Omnicam Scanning Technique. Available online: <https://www.youtube.com/watch?v=E5hzbRNK7pk&t=95s> (accessed on 29 November 2021).
36. 3Shape TRIOS Scan Strategy—Full Arch. Available online: [https://www.youtube.com/watch?v=M\\_KbWcCianY&t=126s](https://www.youtube.com/watch?v=M_KbWcCianY&t=126s) (accessed on 29 November 2021).
37. Thanasisuebwong, P.; Kulchotirat, T.; Anunmana, C. Effects of inter-implant distance on the accuracy of intraoral scanner: An in vitro study. *J. Adv. Prosthodont.* **2021**, *13*, 107–116. [CrossRef] [PubMed]
38. Miyoshi, K.; Tanaka, S.; Yokoyama, S.; Sanda, M.; Baba, K. Effects of different types of intraoral scanners and scanning ranges on the precision of digital implant impressions in edentulous maxilla: An in vitro study. *Clin. Oral Implant. Res.* **2020**, *31*, 74–83. [CrossRef]
39. Mizumoto, R.M.; Alp, G.; Özcan, M.; Yılmaz, B. The effect of scanning the palate and scan body position on the accuracy of complete-arch implant scans. *Clin. Implant. Dent. Relat. Res.* **2019**, *21*, 987–994. [CrossRef]
40. Schmidt, A.; Billig, J.W.; Schlenz, M.A.; Wöstmann, B. The influence of using different types of scan bodies on the transfer accuracy of implant position: An in vitro study. *Int. J. Prosthodont.* **2021**, *34*, 254–260. [CrossRef]
41. Kim, R.J.Y.; Benic, G.I.; Park, J.M. Trueness of digital intraoral impression in reproducing multiple implant position. *PLoS ONE* **2019**, *14*, e0222070. [CrossRef]
42. Mangano, F.G.; Hauschild, U.; Veronesi, G.; Imburgia, M.; Mangano, C.; Admakin, O. Trueness and precision of 5 intraoral scanners in the impressions of single and multiple implants: A comparative in vitro study. *BMC Oral Health* **2019**, *19*, 101. [CrossRef]
43. Braian, M.; Wennerberg, A. Trueness and precision of 5 intraoral scanners for scanning edentulous and dentate complete-arch mandibular casts: A comparative in vitro study. *J. Prosthet. Dent.* **2019**, *122*, 129–136. [CrossRef]
44. Moura, R.V.; Kojima, A.N.; Saraceni, C.H.C.; Bassolli, L.; Balducci, I.; Özcan, M.; Mesquita, A.M.M. Evaluation of the accuracy of conventional and digital impression techniques for implant restorations. *J. Prosthodont.* **2019**, *28*, 530–535. [CrossRef] [PubMed]